Memristive Ising circuits

Vincent J. Dowling and Yuriy V. Pershin*
Department of Physics and Astronomy, University of South Carolina, Columbia, South Carolina 29208, USA

(Received 26 July 2022; accepted 10 November 2022; published 30 November 2022)

The Ising model is of prime importance in the field of statistical mechanics. Here we show that Ising-type interactions can be realized in periodically driven circuits of stochastic binary resistors with memory. A key feature of our realization is the simultaneous coexistence of ferromagnetic and antiferromagnetic interactions between two neighboring spins—an extraordinary property not available in nature. We demonstrate that the statistics of circuit states may perfectly match the ones found in the Ising model with ferromagnetic or antiferromagnetic interactions, and, importantly, the corresponding Ising model parameters can be extracted from the probabilities of circuit states. Using this finding, the Ising Hamiltonian is reconstructed in several model cases, and it is shown that different types of interaction can be realized in circuits of stochastic memristors.

DOI: 10.1103/PhysRevE.106.054156

I. INTRODUCTION

The utilization of electronic circuits as an analog to other physical systems is becoming more and more prevalent. It has been recently shown that certain circuits composed of only capacitors and inductors [1,2] as well as circuits combining passive resistive [3,4] or active [5] components with capacitors and inductors can be used to realize the same states that are found in topological phases in condensed matter [6–9], forming a connection between two otherwise distinct systems. For instance, in the topoelectric Su-Schrieffer-Heeger (SSH) circuit [1] the boundary resonances in the impedance are reminiscent of edge states in the SSH model. Here, we introduce a circuit of stochastic memristors (resistors with memory) exhibiting the same statistics of states as in the Ising model.

While the concept of constructing an electric analog to the Ising model is not novel [10–18] and is gaining increasing attention in the context of building Ising machines [11–18], this paper provides an alternative approach. The basic idea is as follows. We use a resistor and stochastic memristor connected in series as a memristive spin [Fig. 1(a)] and couple memristive spins by resistors to induce their interactions [see Fig. 1(b) for the circuit considered in this paper]. It is assumed that the stochastic memristor can be found in one of two states, $R_{\rm ON}$ and $R_{\rm OFF}$ (such that $R_{\rm ON} < R_{\rm OFF}$), and the switching between these states occurs probabilistically and is described by voltage-dependent switching rates (the details of the model are given below). The circuit is subjected to alternating polarity pulses that drive the memristive dynamics. The states of memristors are read during each period of the pulse sequence (say, at the end of the negative pulse), and the probabilities of these states are determined. We note that the circuit in Fig. 1(b) but with deterministic memristors was introduced in Ref. [19], and a mean-field model of memristive interactions in a similar (but not the same) deterministic circuit was developed in Ref. [20].

Using numerical simulations, we have found that our circuit is capable of exhibiting an analogous type of ordering in memristor configurations to that found in magnetic materials. This means that there can exist a strong bias for a specific circuit to exist in an antiferromagnetic (AFM) memristor configuration (-$R_{\rm ON}$-$R_{\rm OFF}$-$R_{\rm ON}$-$R_{\rm OFF}$-) or an ferromagnetic (FM) memristor configuration (-$R_{\rm ON}$-$R_{\rm ON}$-$R_{\rm ON}$-$R_{\rm ON}$- or -$R_{\rm OFF}$-$R_{\rm OFF}$-$R_{\rm OFF}$-$R_{\rm OFF}$-). In fact, a very important aspect of our circuit is the simultaneous coexistence of AFM and FM interactions between two neighboring spins. The goal of this work is to demonstrate the possibility of the standard magnetic orderings (AFM and FM) in the memristive Ising circuits.

This paper is organized as follows. In Sec. II we introduce the Ising Hamiltonian and the stochastic model of memristors and make the connection between the statistical properties of the circuit and ones of the Ising Hamiltonian. In the same section, we briefly discuss the numerical approach used in this paper. The results of our simulations are presented in Sec. III with the emphasis on the possibility of reaching FM and AFM interactions in the circuit. The paper ends with conclusions in Sec. IV.

II. METHODS

Mathematically, we utilize an effective Ising-type Hamiltonian to describe the probabilities observed in the circuit simulations. For the circuit in Fig. 1(b), the Hamiltonian has the form

$$H = -J\sum_i \sigma_i\sigma_{i+1} - J_2\sum_i \sigma_i\sigma_{i+2} - h\sum_i \sigma_i, \qquad (1)$$

where J is the interaction coefficient for adjacent spins, J_2 is the next-to-adjacent interaction, h is the magnetic field, and periodic coupling is assumed. Schematically, these interactions are presented in Fig. 1(c). We consider the electronic circuit as a physical system described by the Boltzmann

*pershin@physics.sc.edu

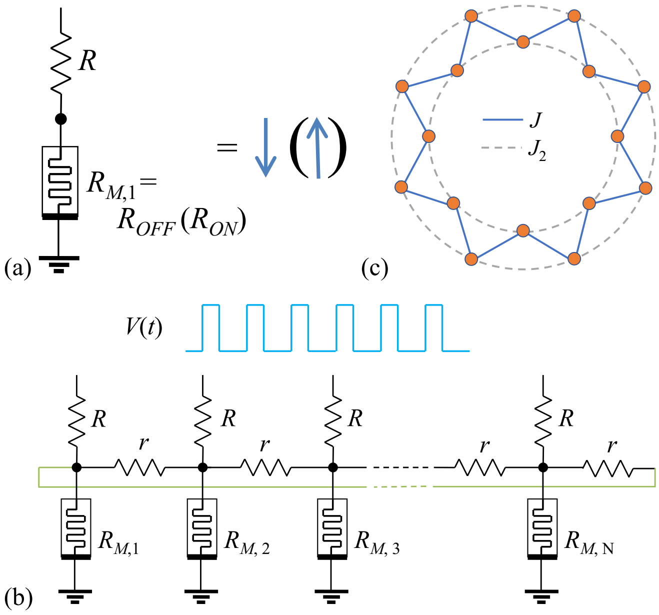

FIG. 1. (a) Memristive spin subcircuit: the high- and low-resistance states of a stochastic memristor correspond to spin-down (0) and spin-up (1) states, respectively. (b) One-dimensional memristive Ising circuit with a periodic boundary condition. Here, r's denote the resistance of coupling resistors. (c) The scheme of interactions in the Ising Hamiltonian.

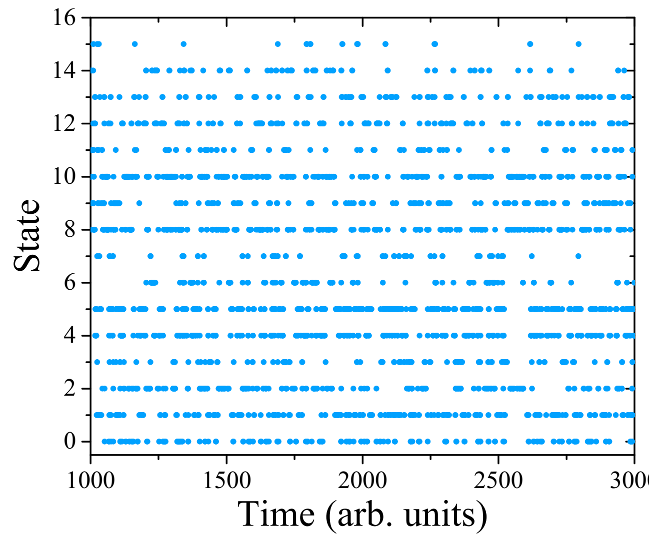

FIG. 2. Dynamics of the states in a circuit with $N = 4$ memristive spins. The circuit has $2^4 = 16$ states that are labeled from 0 to 15. The 0000 state (all memristors are in $R_{\rm OFF}$) is labeled by 0, the 0001 state is labeled by 1, and so on. This plot was obtained using the following set of parameters: $R = r = R_{\rm OFF} = 1$ kΩ, $R_{\rm ON} = 100$ Ω, $\tau_{01} = 3 \times 10^5$ s, $\tau_{10} = 160$ s, $V_{01} = 0.05$ V, $V_{10} = 0.5$ V, $V_{\rm peak} = 1$ V, and $T = 2$ s.

distribution

$$p_i = \frac{1}{Z} e^{-\frac{E_i}{kT}}. \tag{2}$$

Here, $Z = \sum_j e^{-\frac{E_j}{kT}}$ is the statistical sum, and E_j's are the "energies" of circuit states. We argue that for the circuit in Fig. 1 and similar circuits these "energies" correspond to the Ising Hamiltonian (1).

To explain the coexistence of AFM and FM interactions, consider a set of identical memristors in $R_{\rm OFF}$ subjected to a positive voltage pulse driving the OFF-to-ON transition. Each memristor will have an equivalent probability of being the first to switch states. When one of these memristors swaps states, it reduces the probability of its neighbors switching (reducing the voltage across them). In this scenario, memristors with neighbors both in the $R_{\rm OFF}$ state will have the highest chance of switching. This leads to the tendency of antiferromagnetic ordering in the memristors under a positive voltage pulse. However, under a negative voltage pulse the $R_{\rm ON}$ state memristors with neighboring $R_{\rm OFF}$ state memristors will be favored to change states. This means that the configuration will tend towards ferromagnetic ordering under a negative voltage pulse. The overall ordering of a memristive circuit driven by an ac source will then be dependent on the choice of model parameters for the memristors. Based on the parameters, one type of ordering may be dominant.

Next, we introduce the model of stochastic memristors. According to experiments with certain electrochemical metallization (ECM) cells [21,22] and valence change memory (VCM) cells [23], the probability of switching between resistance states of these devices can be described by switching rates of the form

$$\gamma_{0\to1}(V) = \begin{cases} \left(\tau_{01} e^{-V/V_{01}}\right)^{-1} & \text{for } V > 0 \\ 0 & \text{otherwise,} \end{cases} \tag{3}$$

$$\gamma_{1\to0}(V) = \begin{cases} \left(\tau_{10} e^{-|V|/V_{10}}\right)^{-1} & \text{for } V < 0 \\ 0 & \text{otherwise,} \end{cases} \tag{4}$$

where V is the voltage across the device and $\tau_{01(10)}$ and $V_{01(10)}$ are device-specific parameters. Here, 0 and 1 correspond to the high-resistance ($R_{\rm OFF}$) and low-resistance ($R_{\rm ON}$) states, respectively. Under a constant voltage, the probability of switching follows the distribution [21,22]

$$P(t) = \frac{\Delta t}{\tau(V)} e^{-t/\tau(V)}, \tag{5}$$

where $\tau(V)$ is the inverse of the switching rate given by Eqs. (3) or (4) (depending on the sign of V). Previously, we have developed a master equation approach for the circuit of stochastic memristors [24] and designed its implementation in Simulation Program with Integrated Circuit Emphasis (SPICE) [25].

Most of the results presented here are obtained through numerical simulations of the circuit in Fig. 1(b) containing N memristive spins. The set of parameters defining the circuit and the simulations such as the model constants, voltage period, duration, resistances, etc., are first set. The memristors are then initialized to their starting states (typically all OFF). The voltages across each memristor are calculated for the current time step through Kirchhoff's laws. The switching time is then generated for each memristor randomly with the Eq. (5) distribution. The fastest switching time is extracted and compared with the remaining time in the current voltage pulse. If there is sufficient time remaining in the pulse, that

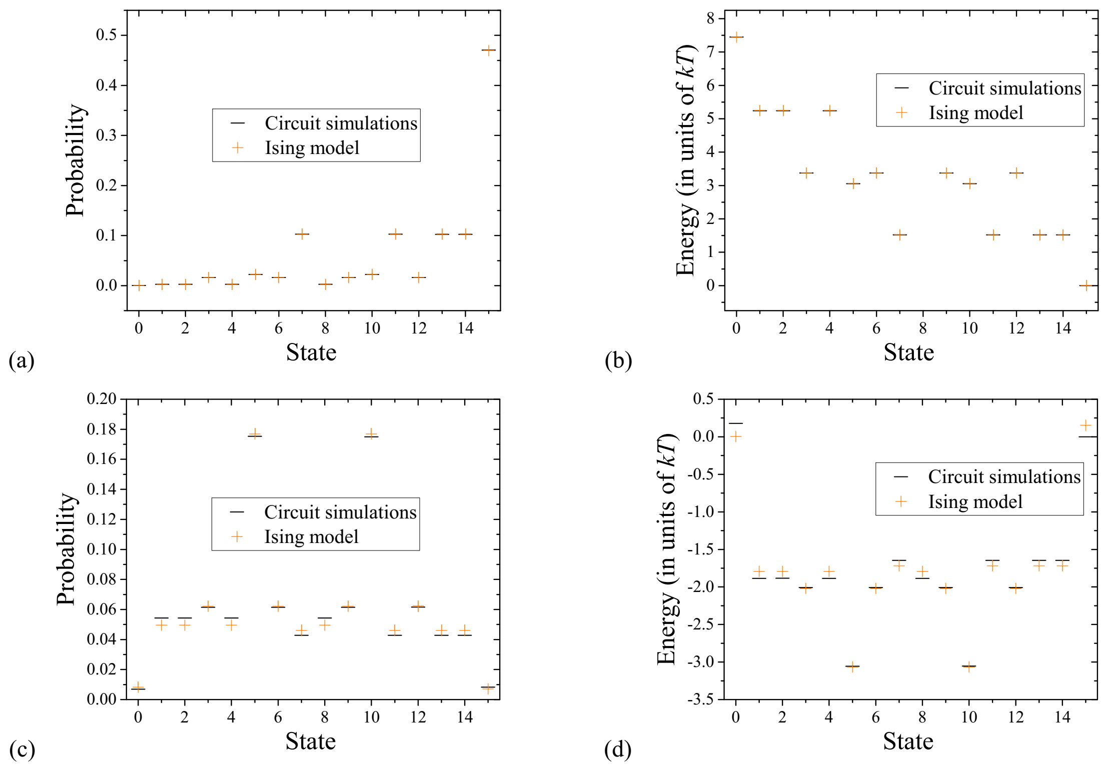

FIG. 3. Comparison of the probabilities and energies found through a $N = 4$ memristor circuit with the values found through the memristor-Ising model for the cases of (a) and (b) a weaker coupling ($r = 10$ kΩ) and (c) and (d) a stronger coupling ($r = 1$ kΩ). Other simulation parameters are the same as in Fig. 2. For (a), the weaker coupling, coefficient values of $J/kT = -0.083\,994\,4$, $h/kT = 0.930\,417$, and $J_2/kT = -0.001\,566\,5$ were found and used. For (b) and (d), the stronger coupling, coefficient values of $J/kT = -0.195\,313$, $h/kT = 1.358\,07$, and $J_2/kT = -0.024\,651$ were found and used.

memristor switches states, and the the time remaining in the period is decreased. The switching times are generated again. If not, the circuit remains in the same state, and the interval of the opposite voltage polarity starts. The simultaneous memristor switchings are not considered as their probability is negligible.

After a sufficient period of time for the circuit to reach a dynamical steady state has passed, the memristor configuration will be tracked for each period of the applied voltage. Once the simulation has been completed, probabilities for every possible memristor configuration will be found using the distribution of configurations from the simulation. These probabilities can then be utilized to calculate "energies" corresponding to the circuit dynamics using Eq. (2).

III. RESULTS

A. FM and AFM couplings

Figure 2 presents an example of state dynamics in the circuit with four memristive spins. One can notice that (on average) the states with antiferromagnetic spin arrangements (such as 5 = 0101b, 10 = 1010b, where b denotes base 2 notation) are more occupied compared with the ferromagnetic states (e.g., 6 = 0110b, 3 = 0011b, etc.). Consequently, the probability for the antiferromagnetic states is higher, and thus one can make the qualitative conclusion that this specific circuit (including the parameters of the driving sequence) is described by the AFM model ($J < 0$).

The Ising model parameters, J, J_2, and h, were found by minimizing the squared difference between the Ising model energies and circuit energies. The latter were obtained based on Eq. (2), which was transformed to $E_i = E_0 - kT\ln(p_i/p_0)$. In the Supplemental Material (SI) [26] we provide explicit relations that were used in the calculation of the constants in the Ising Hamiltonian [Eq. (1)]. Figure 3 shows a comparison between the probabilities and energies of the circuit states (found numerically) and ones calculated based on the Ising model. We observed an excellent agreement in the case of a weaker coupling ($r = 10$ kΩ) and very good agreement in the stronger-coupling case ($r = 1$ kΩ).

The main result of this paper can be seen in Fig. 4. The figure shows how J, J_2, and h vary in relation to the size of the coupling resistance between memristive spins. Clear ferromagnetic and antiferromagnetic ordering can be seen depending on the choice of circuit parameters. These results can be easily extended to circuits with distinct resistances and memristor parameters. For instance, in Fig. 5 we present Ising model parameters found for a circuit with distinct coupling resistances r. Since a memristive spin has a stronger influence on its neighbors when the coupling resistance is smaller, smaller coupling resistances result in larger Ising coefficient J_i (in Fig. 5, r_i and J_i are shifted by 0.5 to the right to emphasize their role in the spin-spin interaction).

In general, circuits can be set to prefer a specific ordering through the selection of the model parameters V_{01} and V_{10}. These parameters, in a sense, set how susceptible a

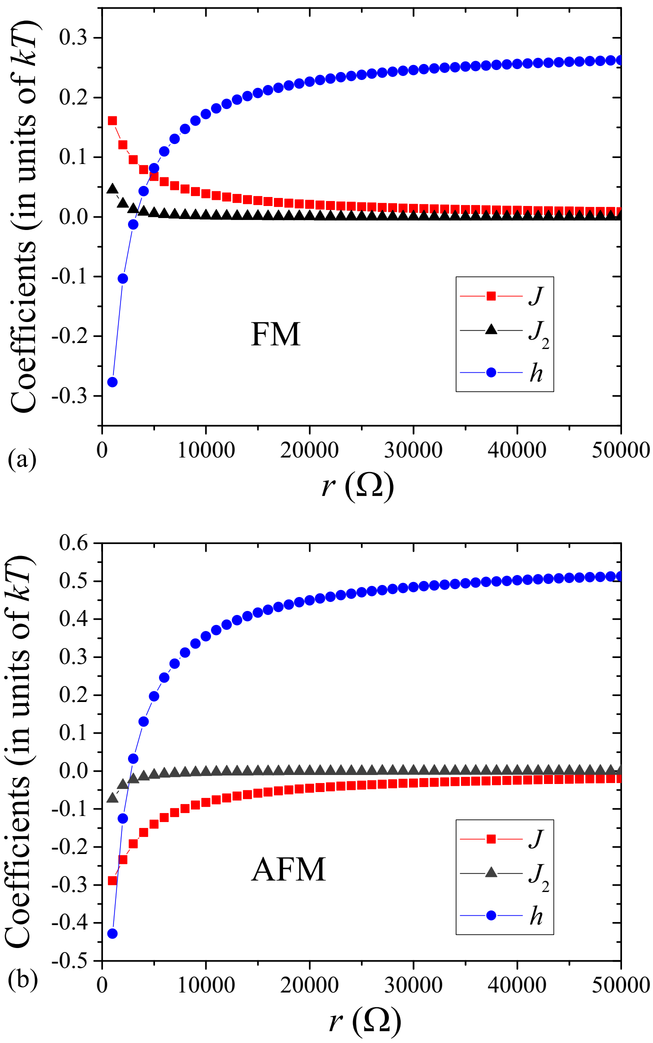

FIG. 4. Comparison of Ising coefficients using two different sets of model parameters as the coupling resistance r is varied showing (a) FM and (b) AFM interactions of memristive spins. The common parameters are $N = 10$, $R = 1$ kΩ, $R_{ON} = 500$ Ω, $R_{OFF} = 2000$ Ω, $V_{peak} = 1$ V, and $T = 2$ s. In (a) we used $\tau_{01} = 160$ s, $\tau_{10} = 6 \times 10^4$ s, $V_{01} = 0.5$ V, and $V_{10} = 0.05$ V. In (b) we used $\tau_{01} = 10^7$ s, $\tau_{10} = 100$ s, $V_{01} = 0.05$ V, and $V_{10} = 0.5$ V.

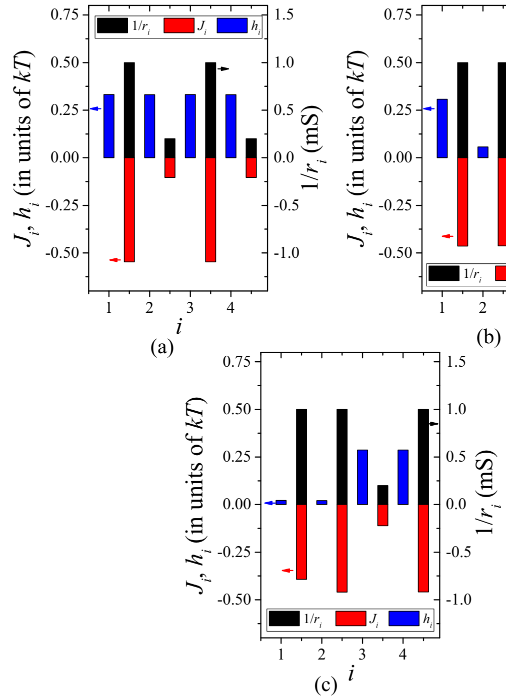

FIG. 5. Ising model parameters for an $N = 4$ circuit with distinct coupling resistances r_i: (a) $r_1 = r_3 = 1$ kΩ, $r_2 = r_4 = 5$ kΩ; (b) $r_1 = r_2 = 1$ kΩ, $r_3 = r_4 = 5$ kΩ; and (c) $r_1 = r_2 = r_4 = 1$ kΩ, $r_3 = 5$ kΩ. All other simulation parameters are the same as in Fig. 2.

memristor is to the states of its neighbors. As memristors switch between resistance states, they induce changes in not only the voltage across themselves, but also the voltages across (in principle) all memristors in the chain in accordance with Kirchoff's circuit laws. The strength of the induced change, or the interaction, weakens as the distance increases from the switching memristor. Through the interplay of the induced changes in the voltages and the chosen set of model parameters, there will be a bias towards a specific type of ordering.

Figure 6(a) shows the dependency of the Ising coefficients on the amount of memristive spins included within a circuit. Here we can see that at five units any major dependency on the amount of units within a circuit disappears. In order to demonstrate the importance of the J_2 interaction in the memristor-Ising Hamiltonian, Fig. 6(b) shows a comparison of approximations with and without J_2. It is clear that J_2 improves the description only in the stronger-coupling case (smaller r's).

B. Comparison with other methods

As a means of verifying the results seen through numerical simulations, a couple of different methods were employed. For specific cases, meaning specific circuit configurations (generally simplistic), exact solutions can be found for the state probabilities in the master equation [24]. These results were then compared with the output of the Monte Carlo simulations to check for agreement. The first method used was exactly solving the master equation analytically through MATHEMATICA. The model parameters were set, the number of memristors was defined, and all possible memristor voltages for any possible configuration were listed. The switching rates then were constructed for any potential circuit configuration or transition. Using these rates, the master equation was solved exactly for the steady state [27], and the probabilities for each type of memristor configuration were found. The second method used was implementing the master equation in SPICE and using the SPICE environment to find the probabilities for each type of memristor configuration. We have obtained an excellent agreement between the results obtained with different methods (see SI for details).

In order to show agreement, one of the specific configurations considered and directly solved through various means was the circuit in Fig. 1(b) containing specifically four memristor-resistor units. This circuit was numerically solved,

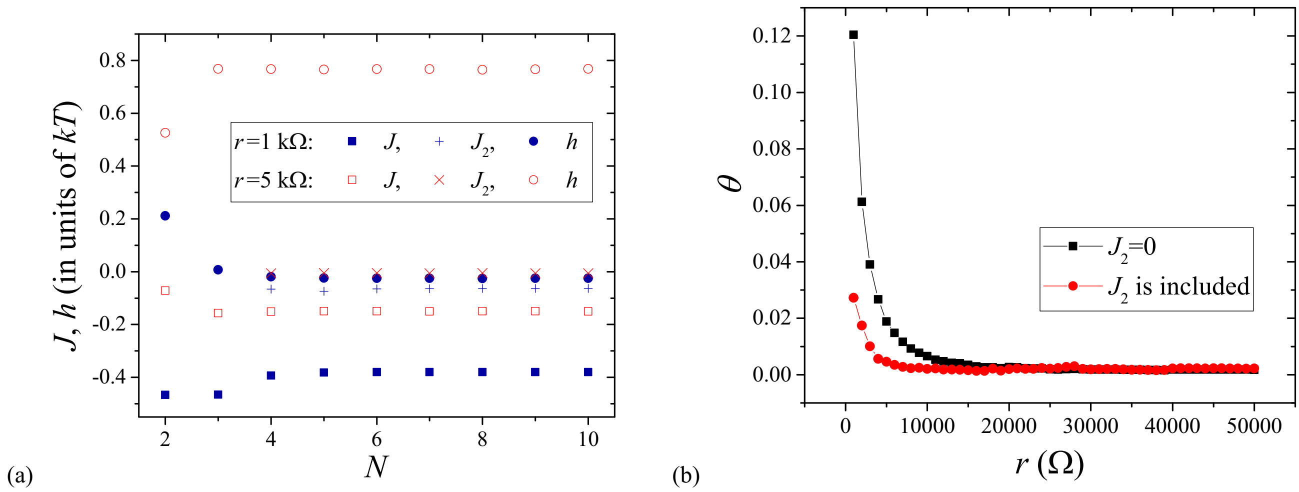

FIG. 6. (a) Change in the Ising coefficients, J, J_2, and h, as the amount of memristive spins in the circuit is varied from $N = 2$ to $N = 10$. The simulation parameters are the same as in Fig. 2. (b) Comparison of the accuracy of the memristor-Ising Hamiltonian with and without J_2 using the dot product of the circuit and Ising model probabilities. This plot shows the angle between vectors of state probabilities. Performed for the case of AFM calculations in Fig. 4 with $N = 5$.

and the master equation was utilized through two applications in order to verify the results obtained by numerical means. In general, the master equation is written as

$$\frac{dp_\Theta(t)}{dt} = \sum_{m=1}^{N} \left(\gamma_{\Theta_m}^{m} p_{\Theta_m}(t) - \gamma_{\Theta}^{m} p_\Theta(t)\right), \tag{6}$$

where p is the probability of being in a specific configuration and γ is the transition rate between configurations. For the specific case of a circuit with four memristor-resistor units the master equation becomes a set of six differential equations with forms of (for a fully detailed application of the master equation, see Ref. [24])

$$\frac{dp_{0000}(t)}{dt} = -4\gamma_{0000}^{1} p_{0000} + 4\gamma_{0001}^{1} p_{0001}. \tag{7}$$

These differential equations, in conjunction with specific memristor voltages for each possible configuration, can be fully solved in MATHEMATICA, and the resulting probabilities for each configuration can be found. A secondary approach is constructing these differential equations in SPICE using a current-controlled voltage source and capacitor pair for each probability along with the full circuit constructed for each memristor configuration [25]. Supplemental Table S1 shows the probability results for this circuit configuration utilizing the same parameters for all three types of analysis.

IV. CONCLUSION

In conclusion, research into electronic systems that can replicate the statistics of the Ising model or other statistical systems is of increasing interest. In this paper, we have demonstrated that circuits constructed with memristor-resistors units are capable of serving as an analog for the switching behavior exhibited by the Ising model. Our results show an almost perfect match between the energies and probabilities that one would expect from the Ising Hamiltonian and those obtained from the numerical simulations performed here. We show the small-to-negligible gain in accuracy for including interaction terms beyond the first neighbor. The results from these simulations were further verified by other forms of analysis. Finally, it is shown that both types of orderings, ferromagnetic and antiferromagnetic, can be realized in these circuits under the appropriate set of model parameters. Experimental implementations of the circuits studied would be useful, but they are beyond the scope of this paper. This work further adds to the class of electronic circuits that are capable of realizing the behavior of other physical systems.

[1] C. H. Lee, S. Imhof, C. Berger, F. Bayer, J. Brehm, L. W. Molenkamp, T. Kiessling, and R. Thomale, Topolectrical circuits, Commun. Phys. **1**, 39 (2018).
[2] S. Imhof, C. Berger, F. Bayer, J. Brehm, L. W. Molenkamp, T. Kiessling, F. Schindler, C. H. Lee, M. Greiter, T. Neupert, and R. Thomale, Topolectrical-circuit realization of topological corner modes, Nat. Phys. **14**, 925 (2018).
[3] T. Hofmann, T. Helbig, F. Schindler, N. Salgo, M. Brzezinska, M. Greiter, T. Kiessling, D. Wolf, A. Vollhardt, A. Kabasi, C. H. Lee, A. Bilusic, R. Thomale, and T. Neupert, Reciprocal skin effect and its realization in a topolectrical circuit, Phys. Rev. Res. **2**, 023265 (2020).
[4] M. Di Ventra, Y. V. Pershin, and C.-C. Chien, Custodial Chiral Symmetry in a Su-Schrieffer-Heeger Electrical Circuit with Memory, Phys. Rev. Lett. **128**, 097701 (2022).
[5] T. Kotwal, F. Moseley, A. Stegmaier, S. Imhof, H. Brand, T. Kießling, R. Thomale, H. Ronellenfitsch, and J. Dunkel, Active topolectrical circuits, Proc. Natl. Acad. Sci. USA **118**, e2106411118 (2021).

[6] J. K. Asbóth, L. Oroszlány, and A. Pályi, *A Short Course on Topological Insulators: Band-Structure Topology and Edge States in One and Two Dimensions* (Springer, Berlin, 2016).
[7] S.-Q. Shen, *Topological Insulators: Dirac Equation in Condensed Matters* (Springer, Berlin, 2012).
[8] T. Tuloup, R. W. Bomantara, C. H. Lee, and J. Gong, Nonlinearity induced topological physics in momentum space and real space, Phys. Rev. B **102**, 115411 (2020).
[9] Y. Hadad, A. B. Khanikaev, and A. Alu, Self-induced topological transitions and edge states supported by nonlinear staggered potentials, Phys. Rev. B **93**, 155112 (2016).
[10] I. Mahboob, H. Okamoto, and H. Yamaguchi, An electromechanical Ising Hamiltonian, Sci. Adv. **2**, e1600236 (2016).
[11] N. A. Aadit, A. Grimaldi, M. Carpentieri, L. Theogarajan, J. M. Martinis, G. Finocchio, and K. Y. Camsari, Massively parallel probabilistic computing with sparse Ising machines, Nat. Electron. **5**, 460 (2022).
[12] W. A. Borders, A. Z. Pervaiz, S. Fukami, K. Y. Camsari, H. Ohno, and S. Datta, Integer factorization using stochastic magnetic tunnel junctions, Nature (London) **573**, 390 (2019).
[13] B. Sutton, K. Y. Camsari, B. Behin-Aein, and S. Datta, Intrinsic optimization using stochastic nanomagnets, Sci. Rep. **7**, 44370 (2017).
[14] J. Chou, S. Bramhavar, S. Ghosh, and W. Herzog, Analog coupled oscillator based weighted Ising machine, Sci. Rep. **9**, 14786 (2019).
[15] S. Dutta, A. Khanna, J. Gomez, K. Ni, Z. Toroczkai, and S. Datta, Experimental demonstration of phase transition nano-oscillator based Ising machine, in *2019 IEEE International Electron Devices Meeting (IEDM)* (IEEE, Piscataway, NJ, 2019), pp. 37.8.1–37.8.4.
[16] S. Dutta, A. Khanna, A. Assoa, H. Paik, D. G. Schlom, Z. Toroczkai, A. Raychowdhury, and S. Datta, An Ising Hamiltonian solver based on coupled stochastic phase-transition nano-oscillators, Nat. Electron. **4**, 502 (2021).
[17] F. Cai, S. Kumar, T. Van Vaerenbergh, X. Sheng, R. Liu, C. Li, Z. Liu, M. Foltin, S. Yu, Q. Xia, J. J. Yang, R. Beausoleil, W. D. Lu, and J. P. Strachan, Power-efficient combinatorial optimization using intrinsic noise in memristor Hopfield neural networks, Nat. Electron. **3**, 409 (2020).
[18] M. N. Bojnordi and E. Ipek, Memristive Boltzmann machine: A hardware accelerator for combinatorial optimization and deep learning, in *2016 IEEE International Symposium on High Performance Computer Architecture (HPCA)* (IEEE, Piscataway, NJ, 2016), pp. 1–13.
[19] V. A. Slipko and Y. V. Pershin, Metastable memristive lines for signal transmission and information processing applications, Phys. Rev. E **95**, 042213 (2017).
[20] F. Caravelli and P. Barucca, A mean-field model of memristive circuit interaction, Europhys. Lett. **122**, 40008 (2018).
[21] S. H. Jo, K.-H. Kim, and W. Lu, Programmable resistance switching in nanoscale two-terminal devices, Nano Lett. **9**, 496 (2009).
[22] S. Gaba, P. Sheridan, J. Zhou, S. Choi, and W. Lu, Stochastic memristive devices for computing and neuromorphic applications, Nanoscale **5**, 5872 (2013).
[23] R. Naous, A. Siemon, M. Schulten, H. Alahmadi, A. Kindsmüller, M. Lübben, A. Heittmann, R. Waser, K. N. Salama, and S. Menzel, Theory and experimental verification of configurable computing with stochastic memristors, Sci. Rep. **11**, 4218 (2021).
[24] V. J. Dowling, V. A. Slipko, and Y. V. Pershin, Probabilistic memristive networks: Application of a master equation to networks of binary ReRAM cells, Chaos Solitons Fractals **142**, 110385 (2021).
[25] V. J. Dowling, V. A. Slipko, and Y. V. Pershin, Modeling networks of probabilistic memristors in SPICE, Radioengineering **30**, 157 (2021).
[26] See Supplemental Material at http://link.aps.org/supplemental/10.1103/PhysRevE.106.054156 for details.
[27] V. J. Dowling, V. A. Slipko, and Y. V. Pershin, Analytic and spice modeling of stochastic ReRAM circuits, in *International Conference on Micro-and Nano-Electronics 2021*, Proceedings of SPIE (SPIE, Bellingham, WA, 2022), Vol. 12157 , pp. 72–80.